FORWARD AND INVERSE KINEMATICS OF DOUBLE UNIVERSAL JOINT ROBOT WRISTS

Dr. Robert L. Williams II
Automation Technology Branch, M.S. 152D
NASA Langley Research Center
Hampton, VA 23665-5225

ABSTRACT

A robot wrist consisting of two universal joints can eliminate the wrist singularity problem found on many industrial robots. This paper presents forward and inverse position and velocity kinematics for such a wrist having three degrees of freedom. Denavit-Hartenberg parameters are derived to find the transforms required for the kinematic equations. The Omni-Wrist, * a commercial double universal joint robot wrist, is studied in detail. There are four levels of kinematic parameters identified for this wrist; three forward and three inverse maps are presented for both position and velocity. These equations relate the hand coordinate frame to the wrist base frame. They are sufficient for control of the wrist standing alone.

When the wrist is attached to a manipulator arm, the offset between the two universal joints complicates the solution of the overall kinematics problem. All wrist coordinate frame origins are not coincident, which prevents decoupling of position and orientation for manipulator inverse kinematics. This is a topic for future research.

INTRODUCTION

Many current industrial robot wrists suffer from singularity limitations where at least two wrist coordinate frames align, reducing orientational freedom. Near singular positions, extremely large joint rates are required to maintain constant cartesian rates. One proposed wrist design for reducing singularities uses the universal joint to achieve roll, pitch, and yaw orientation. An overview of robot wrists, including universal joint designs, is given by Rosheim (1989). Other references present non-singular robot wrist designs, e.g., (Barker, 1986), (Milenkovic, 1987), (Rosheim, 1987 and 1986), and (Trevelyan, 1986).

McKinney (1988) presents forward kinematic and resolved rate equations for single and double universal joint robot wrists. The author studies a specific double universal joint wrist, the Omni-Wrist from Ross-Hime Designs, Inc. A single universal joint wrist is attractive because its motion is purely rotational. However, the workspace is limited due to gimbal lock singularities. Also, the roll velocity of the output shaft is variable, given a constant input roll rate. Therefore, a wrist with two universal joints in series is suggested, which allows an approximately hemispherical singularity-free workspace (McKinney, 1988). Two universal joints yield a constant roll velocity ratio (Mabie and Reinholtz, 1987).

The current paper presents forward and inverse kinematic position and velocity equations for control of double universal joint robot wrists. Denavit-Hartenberg parameters are presented for double universal joint wrists. The Omni-Wrist kinematic transformations are presented. Four levels of kinematic parameters are identified, from the actuator angles to the position and orientation of the hand. Three mappings are presented for each of the forward position, inverse position, forward velocity, and inverse velocity (resolved rate) problems. These equations relate the robot hand to the robot wrist base and are sufficient for control of the wrist standing alone.

The double universal joint wrist is not purely rotational due to the offset between the two universal joints. Position and orientation trajectories thus may not be decoupled for a double universal joint wrist attached to a manipulator arm. The manipulator inverse position and velocity problems are more complicated for the double universal joint robot wrist than a purely rotational robot wrist.

* The mention herein of a trademark of a commercial product does not constitute any recommendation for use by the Government.

SYMBOLS

$\{m\}$	Cartesian coordinate frame m
$\{3\}$	Wrist base coordinate frame
$\{8\}$	Hand coordinate frame
$\theta_{4A}, \theta_{5A}, \theta_{6A}$	Actuator angles
$\theta_{4G}, \theta_{5G}, \theta_{6G}$	Gear bail angles
$\theta_4, \theta_5, \theta_6$	Universal joint angles
$[{}^n_m T]$	Homogeneous transformation matrix of $\{m\}$ relative to $\{n\}$
$[{}^n_m R]$	Rotation matrix of $\{m\}$ relative to $\{n\}$
r_{ij}	Element (i,j) of $[{}^3_8 R]$
$\{{}^n P_m\}$	Position vector from origin of $\{n\}$ to $\{m\}$, expressed in $\{n\}$
$\{{}^n \hat{X}_m\}$	Unit direction vector X of $\{m\}$ expressed in $\{n\}$
$\{{}^m \omega_m\}$	Angular velocity of $\{m\}$ with respect to $\{3\}$, expressed in $\{m\}$
$\{{}^m v_m\}$	Linear velocity of $\{m\}$ origin with respect to $\{3\}$, expressed in $\{m\}$
$F1$	Forward map solving θ_{iG} given θ_{iA}, i=4,5,6
$F2$	Forward map solving θ_i given θ_{iG}, i=4,5,6
$F3$	Forward map solving $[{}^3_8 T]$ given θ_i, i=4,5,6
$I1, I2, I3$	Inverses of $F3, F2, F1$, respectively
$FVi, IVi, i = 1, 2, 3$	Forward and Inverse velocity maps, defined analogously
$\dot{\theta}_i$	Joint rate i
c_i	$cos\theta_i$
s_i	$sin\theta_i$
t_i	$tan\theta_i$
L	Offset length between the universal joints

DOUBLE UNIVERSAL JOINT WRIST KINEMATICS

A universal joint is used to transfer rotations between intersecting shafts. Most kinematics textbooks discuss universal joints (e.g. Mabie and Reinholtz, 1987). A kinematic diagram for the double universal joint robot wrist is shown in Fig. 1. The input shaft rotates about a fixed axis and the output shaft is free; thus there are five degrees of freedom. Coupling of θ_5 and θ_6 reduces this number to three degrees of freedom.

Figure 1 shows the initial position for all wrist coordinate frames; all universal joint angles are zero in this configuration. Frame {3} is the wrist base frame, fixed for this paper. Frame {4} rotates by θ_4 relative to {3}; {5} rotates by θ_5 relative to {4}; {6} rotates by θ_6 relative to {5}; {7} rotates by the coupled θ_6 relative to {6}; and the hand frame {8} rotates by the coupled θ_5 relative to {7}.

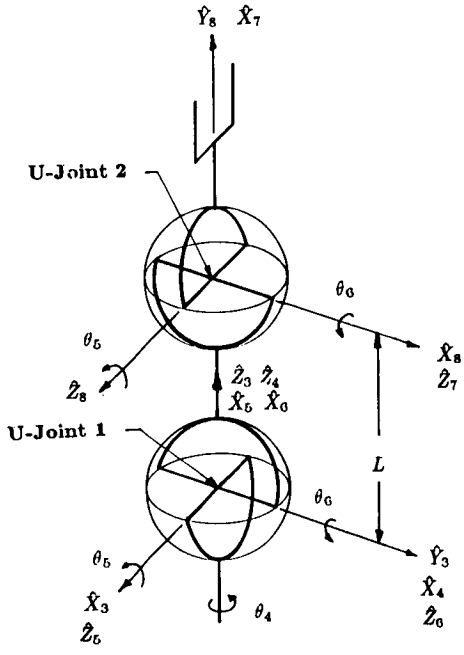

Figure 1
Double Universal Joint Robot Wrist Kinematic Diagram

Denavit-Hartenberg Parameters

The Denavit-Hartenberg parameters for the double universal joint robot wrist of Fig. 1 are given in Table I, which follows the convention in Craig (1988).

Table I Denavit-Hartenberg Parameters

i	α_{i-1}	a_{i-1}	d_i	θ_i
4	0	0	0	$\theta_4 + 90°$
5	90°	0	0	$\theta_5 + 90°$
6	90°	0	0	θ_6
7	0	L	0	θ_6
8	-90°	0	0	$\theta_5 - 90°$

Forward Position

The forward solution finds $[{}^3_8T]$ given θ_4, θ_5, θ_6. Equation 1 is the homogeneous transformation matrix describing the position and orientation of $\{i\}$ with respect to $\{i-1\}$ (Craig, 1988).

$$[{}^{i-1}_{i}T] = \begin{bmatrix} c\theta_i & -s\theta_i & 0 & a_{i-1} \\ s\theta_i c\alpha_{i-1} & c\theta_i c\alpha_{i-1} & -s\alpha_{i-1} & -d_i s\alpha_{i-1} \\ s\theta_i s\alpha_{i-1} & c\theta_i s\alpha_{i-1} & c\alpha_{i-1} & d_i c\alpha_{i-1} \\ 0 & 0 & 0 & 1 \end{bmatrix} \quad (1)$$

Five homogeneous transformation matrices relating {3} through {8} are obtained by substituting the Denavit-Hartenberg parameters into Eq. 1.

$$[{}^3_4T] = \begin{bmatrix} -s_4 & -c_4 & 0 & 0 \\ c_4 & -s_4 & 0 & 0 \\ 0 & 0 & 1 & 0 \\ 0 & 0 & 0 & 1 \end{bmatrix} \quad [{}^4_5T] = \begin{bmatrix} -s_5 & -c_5 & 0 & 0 \\ 0 & 0 & -1 & 0 \\ c_5 & -s_5 & 0 & 0 \\ 0 & 0 & 0 & 1 \end{bmatrix}$$

$$[{}^5_6T] = \begin{bmatrix} c_6 & -s_6 & 0 & 0 \\ 0 & 0 & -1 & 0 \\ s_6 & c_6 & 0 & 0 \\ 0 & 0 & 0 & 1 \end{bmatrix} \quad [{}^6_7T] = \begin{bmatrix} c_6 & -s_6 & 0 & L \\ s_6 & c_6 & 0 & 0 \\ 0 & 0 & 1 & 0 \\ 0 & 0 & 0 & 1 \end{bmatrix}$$

$$[{}^7_8T] = \begin{bmatrix} s_5 & c_5 & 0 & 0 \\ 0 & 0 & 1 & 0 \\ c_5 & -s_5 & 0 & 0 \\ 0 & 0 & 0 & 1 \end{bmatrix}$$

The general forward kinematics solution is Eq. 2. The (4×4) forward transform is comprised of a (3 × 3) rotation matrix representing the orientation and a (3 × 1) position vector locating the origin of {8} in {3}. The specific terms are given in Eq. 3.

$$[{}^3_8T] = \left[\begin{array}{ccc|c} & [{}^3_8R] & & \{{}^3P_8\} \\ \hline 0 & 0 & 0 & 1 \end{array}\right] \quad (2)$$

$$[{}^3_8T] = [{}^3_4T(\theta_4)]\,[{}^4_5T(\theta_5)]\,[{}^5_6T(\theta_6)]\,[{}^6_7T(\theta_6)]\,[{}^7_8T(\theta_5)]$$

$$[{}^3_8T] = \begin{bmatrix} 2s_5c_6K1 - s_4 & 2c_5c_6K1 & -2s_6K1 + c_4 & L(K1) \\ 2s_5c_6K2 + c_4 & 2c_5c_6K2 & -2s_6K2 + s_4 & L(K2) \\ 2s_5c_5c_6^2 & 2c_5^2c_6^2 - 1 & -2c_5s_6c_6 & Lc_5c_6 \\ 0 & 0 & 0 & 1 \end{bmatrix} \quad (3)$$

$$K1 = c_4s_6 + s_4s_5c_6$$

$$K2 = s_4s_6 - c_4s_5c_6$$

Inverse Position

The inverse problem solves for the universal joint angles given task space input. The full $[{}^3_8T]$ cannot be specified because it has six freedoms, and the wrist only three. Due to the following constraint, which dictates that $\{{}^3P_8\}$ travel on the surface of a sphere of radius L, $\{{}^3P_8\}$ cannot be the input, because it has two independent freedoms.

$$P_x^2 + P_y^2 + P_z^2 = L^2 \quad (4)$$

The rotation matrix $[{}^3_8R]$ is the input to the inverse problem.

$$[{}^3_8R] = \begin{bmatrix} r_{11} & r_{12} & r_{13} \\ r_{21} & r_{22} & r_{23} \\ r_{31} & r_{32} & r_{33} \end{bmatrix} \quad (5)$$

$$[{}^3_8R] = [{}^3_4R(\theta_4)]\,[{}^4_5R(\theta_5)]\,[{}^5_6R(\theta_6)]\,[{}^6_7R(\theta_6)]\,[{}^7_8R(\theta_5)]$$

The angle θ_4 is isolated by inverting $[{}^3_4R]$ and multiplying it on the left of both sides of Eq. 5.

$$[{}^3_4R(\theta_4)^{-1}]\,[{}^3_8R] = [{}^4_5R(\theta_5)]\,[{}^5_6R(\theta_6)]\,[{}^6_7R(\theta_6)]\,[{}^7_8R(\theta_5)] \quad (6)$$

The angles θ_5 and θ_6 are eliminated from the right hand side of Eq. 6 by equating the (1,1), (2,3), and (3,2) elements, given in Eqs. 7, 8, and 9, respectively.

$$r_{21}c_4 - r_{11}s_4 = -2s_5^2c_6^2 + 1 \quad (7)$$
$$-r_{13}c_4 - r_{23}s_4 = -2c_6^2 + 1 \quad (8)$$
$$r_{32} = 2c_5^2c_6^2 - 1 \quad (9)$$

Equation 7 is subtracted from Eq. 9 to eliminate θ_5.

$$r_{32} - r_{21}c_4 + r_{11}s_4 = 2c_6^2 - 2 \quad (10)$$

Equations 8 and 10 are added to remove θ_6.

$$\begin{aligned} Ecos\theta_4 + Fsin\theta_4 + G = 0 \\ E = -(r_{13} + r_{21}) \\ F = r_{11} - r_{23} \\ G = r_{32} + 1 \end{aligned} \quad (11)$$

Using the tan half angle substitution (Mabie and Reinholtz, 1987), there are two solutions for θ_4:

$$\theta_{4_{1,2}} = 2tan^{-1}\left[\frac{-F \pm \sqrt{E^2 + F^2 - G^2}}{G - E}\right] \quad (12)$$

The radicand in Eq. 12 is simplified with orthonormal constraints. The columns of $[{}^3_8R]$ are the X, Y, Z unit vectors of $\{8\}$ expressed in $\{3\}$ coordinates, while the rows are those of $\{3\}$ given in $\{8\}$. The orthogonal constraints dictate that both the columns and rows of a rotation matrix form a dextral mutually perpendicular set. The normal constraints dictate that the length of all columns and rows is unity. With the following four constraints, $E^2 + F^2 - G^2 = 0$.

$$\begin{aligned} {}^3\hat{Y}_8 &= {}^3\hat{Z}_8 \times {}^3\hat{X}_8 \\ \left|{}^8\hat{X}_3\right| &= 1.0 \\ \left|{}^3\hat{Y}_8\right| &= 1.0 \\ \left|{}^8\hat{Y}_3\right| &= 1.0 \end{aligned} \quad (13)$$

Therefore, given $[{}^3_8R]$, there is one solution to θ_4 (two repeated roots), from Eq. 12.

$$\theta_4 = 2tan^{-1}\left[\frac{-F}{G - E}\right] \quad (14)$$

With θ_4 solved, the left hand side of Eq. 6 is known. The next step is to isolate and solve θ_5.

$$[{}^4_5R(\theta_5)^{-1}]\,[{}^3_4R(\theta_4)^{-1}]\,[{}^3_8R]\,[{}^7_8R(\theta_5)^{-1}] = [{}^5_6R(\theta_6)]\,[{}^6_7R(\theta_6)] \quad (15)$$

The (2,2) elements of Eq. 15 are equated to solve θ_5.

$$\theta_5 = tan^{-1}\left[\frac{r_{13}s_4 - r_{23}c_4}{r_{33}}\right] \quad (16)$$

Both solutions from the inverse tangent function are mathematically valid, due to symmetry: θ_5 $(\frac{-\pi}{2} < \theta_5 < \frac{-\pi}{2})$ and $\theta_5 + \pi$. When θ_4 and θ_5 are known the left hand side of Eq. 15 is known. Angle θ_6 is solved by equating the (3,2) elements of Eq. 15.

$$2\theta_6 = cos^{-1}\left(r_{13}c_4 + r_{23}s_4\right) \quad (17)$$

The inverse cosine function solution is $\pm 2\theta_6$. This ambiguity is resolved by determining which sign satisfies the (1,2) terms of Eq. 15.

$$s2\theta_6 = (r_{23}c_4 - r_{13}s_4)s_5 - r_{33}c_5 \quad (18)$$

The proper sign for $2\theta_6$ is chosen from Eq. 18. Another valid solution for $2\theta_6$ is $2\theta_6 + 2\pi$; therefore, a second mathematical solution for θ_6 is $\theta_6 + \pi$.

A generalization is drawn regarding the two solutions for θ_5. The right hand side of Eq. 18 for $\theta_5 + \pi$ is the negative of that value for θ_5. Therefore, the value of θ_6 corresponding to $\theta_5 + \pi$ is the negative of θ_6 corresponding to θ_5.

There are four solutions to the inverse problem: a unique θ_4, two θ_5 for this θ_4, plus two θ_6 for each θ_5. Only one combination need be solved; the remaining three are formed from the structure of the solution, summarized in Table II. In rows 1 and 2 of Table II, θ_6 can be positive or negative; the negative θ_6 in rows 3 and 4 indicates opposite sign to θ_6 of row 1 .

Table II Inverse Position Solutions

Solution	θ_4	θ_5	θ_6
1	θ_4	θ_5	θ_6
2	θ_4	θ_5	$\theta_6 + \pi$
3	θ_4	$\theta_5 + \pi$	$-\theta_6$
4	θ_4	$\theta_5 + \pi$	$-\theta_6 + \pi$

Forward Velocity

The forward velocity problem solves for cartesian rates given joint rates using velocity recursion equations (Craig, 1988).

$$\{{}^{i+1}\omega_{i+1}\} = [{}^{i+1}_iR]\{{}^i\omega_i\} + \dot{\theta}_{i+1}\{{}^{i+1}\hat{Z}_{i+1}\} \quad (19)$$
$$\{{}^{i+1}v_{i+1}\} = [{}^{i+1}_iR]\left(\{{}^iv_i\} + \{{}^i\omega_i\} \times \{{}^iP_{i+1}\}\right) \quad (20)$$

The wrist Jacobian matrix is extracted from the forward velocity solution. The (6×3) Jacobian matrix maps the (3×1) joint rates into the (6×1) cartesian rates. The Jacobian matrix is partitioned into (3×3) rotational and translational Jacobian matrices, $[J_R]$ and $[J_T]$.

$$\begin{aligned} \{{}^8\omega_8\} &= [J_R]\{\dot{\theta}\} \\ [J_R] &= \begin{bmatrix} s2\theta_5c_6^2 & s_5s2\theta_6 & 2c_5 \\ 2c_5^2c_6^2 - 1 & c_5s2\theta_6 & -2s_5 \\ -c_5s2\theta_6 & 2c_6^2 & 0 \end{bmatrix} \\ \{\dot{\theta}\} &= \begin{Bmatrix} \dot{\theta}_4 \\ \dot{\theta}_5 \\ \dot{\theta}_6 \end{Bmatrix} \end{aligned} \quad (21)$$

$$\begin{aligned} \{{}^8v_8\} &= [J_T]\{\dot{\theta}\} \\ [J_T] &= L\begin{bmatrix} s_6 & -c_5c_6 & s_5s_6 \\ 0 & s_5c_6 & c_5s_6 \\ s_5c_6 & 0 & c_6 \end{bmatrix} \end{aligned} \quad (22)$$

Inverse Velocity (Resolved Rate)

The resolved rate problem solves for joint rates given cartesian rates. This problem is overconstrained (six equations in three unknowns). Therefore, only three cartesian rates may be specified. The resolved rate input cannot be $\{{}^8v_8\}$ because $[J_T]$ is always singular. This is due to the constraint, Eq. 4.

$$|J_T| = Ls_5s_6c_6^2(1 - c_5^2 - s_5^2) = 0 \quad (23)$$

The inverse velocity problem is solved by inverting Eq. 21.

$$\{\dot{\theta}\} = [J_R^{-1}]\,\{{}^8\omega_8\}$$

$$[J_R^{-1}] = \begin{bmatrix} t_5 & 1 & \frac{-t_6}{c_5} \\ s_5 t_6 & c_5 t_6 & 1 - \frac{1}{2c_5^2} \\ c_5 - \frac{1}{2c_5} & -s_5 & \frac{1}{2} t_5 t_6 \end{bmatrix} \tag{24}$$

The wrist singularity conditions are found by setting the determinant to zero.

$$|J_R| = 4c_5 c_6^2 = 0 \tag{25}$$

The double universal joint robot wrist is singular when $\theta_5 = \pm\frac{\pi}{2}$ or $\theta_6 = \pm\frac{\pi}{2}$.

OMNI-WRIST KINEMATICS

The Omni-Wrist by Ross-Hime Designs, Inc. is a double universal joint robot wrist. Figure 2 displays a section view of the Omni-Wrist. Planetary gears transfer the first universal joint rotations θ_5 and θ_6 to the second universal joint.

The rotational axes for θ_5 and θ_6 are moving. The Omni-Wrist has outer and inner bevel gear bails to transfer rotations from two actuators fixed in the wrist base to the angles θ_5 and θ_6, to avoid moving actuators. No intermediate gear bail is required for θ_4 because it rotates about an axis fixed in the wrist base. In addition to the outer and inner gear bails, helical gear trains are used to reduce the speed and amplify the torque for each of the three actuators.

Referring to Fig. 2, actuator 1 drives θ_4. The inner gear bail rotates in the plane of the paper; the outer rotates about a perpendicular axis. The inner gear bail angle, rotated by actuator 2, equals θ_6 when $\theta_4 = \theta_5 = 0$. Actuator 3 rotates the outer gear bail, whose angle equals θ_5 when $\theta_4 = \theta_6 = 0$. In general, the inner and outer gear bails combine to yield θ_5 and θ_6.

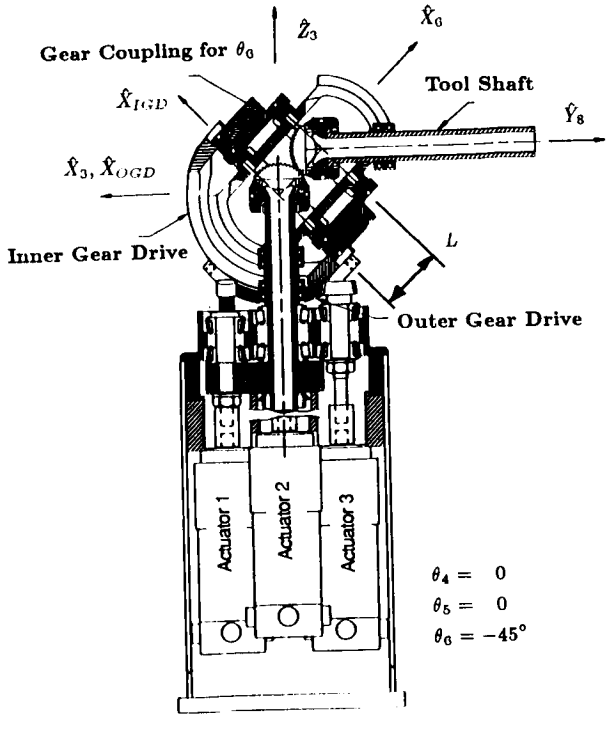

Figure 2
Omni-Wrist Section View

The roll angle θ_4 is continuous and bidirectional. The inner and outer gear bail angles are limited to ±45°. These limits apply to θ_5 when $\theta_4 = \theta_6 = 0$, and to θ_6 when $\theta_4 = \theta_5 = 0$. When these angles are not zero, the limits on θ_5 and θ_6 are more restrictive.

There are four levels of Omni-Wrist kinematic parameters: 1) Actuator angles $(\theta_{4A}, \theta_{5A}, \theta_{6A})$; 2) Gear bail angles $(\theta_{4G}, \theta_{5G}, \theta_{6G})$; 3) Universal joint angles $(\theta_4, \theta_5, \theta_6)$; and 4) Hand coordinate frame $[{}^3_8T]$. All angles are zero in the initial position.

Omni-Wrist Position Kinematics

Figure 3 describes the three forward and inverse position mappings between the four levels of Omni-Wrist kinematic parameters. The overall forward position problem finds $[{}^3_8T]$ given the actuator angles, using maps $F1, F2$, and $F3$. The inverse position problem finds the actuator angles given $[{}^3_8R]$ via the maps $I1, I2$, and $I3$.

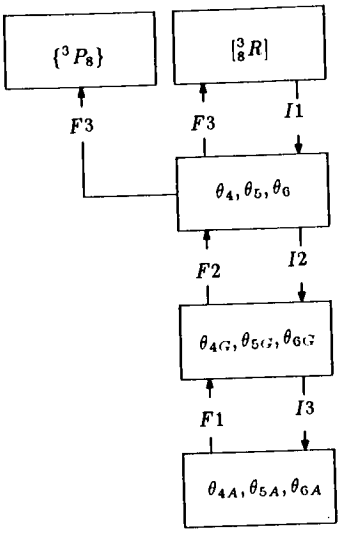

Figure 3
Position Mappings

Maps $F3$ and $I1$ are the general wrist solutions, Eq. 3 and Eqs. 14, 16, and 17, respectively. The remaining maps are developed in this section.

Position Maps $F1$ and $I3$

The gear bail angles are related to the actuator angles by gear trains. Forward map $F1$ is given in Eq. 26.

$$\theta_{4G} = N_1 \theta_{4A} \tag{26a}$$
$$\theta_{5G} = N_2 \theta_{5A} \tag{26b}$$
$$\theta_{6G} = N_3 \theta_{6A} \tag{26c}$$

For the Omni-Wrist, $N_1 = \frac{-1}{175.5}$, $N_2 = \frac{1}{259.2}$, and $N_3 = \frac{-1}{220.0}$. The map $I3$ is the inverse of Eqs. 26.

Position Maps $F2$ and $I2$

The kinematic relationships between the gear bail angles and the universal joint angles are coupled and transcendental. McKinney (1988) solved a problem equivalent to $I2$; the map $F2$ was not solved.

Two coordinate frames are introduced to determine the kinematic relationships between the gear bail and universal joint angles. The $\{IGD\}$ frame is attached to the inner gear bail, and $\{OGD\}$ is attached to the outer gear bail, as shown in Fig. 4. Both origins are colocated with the origin of $\{3\}$. In the initial position, $\{3\}$, $\{IGD\}$, and $\{OGD\}$ are coincident. The inner gear bail rotates by angle θ_{6G} about the fixed axis $\hat{Y}_{IGD}$; the outer gear bail rotates about the fixed $\hat{X}_{OGD}$ by θ_{5G}.

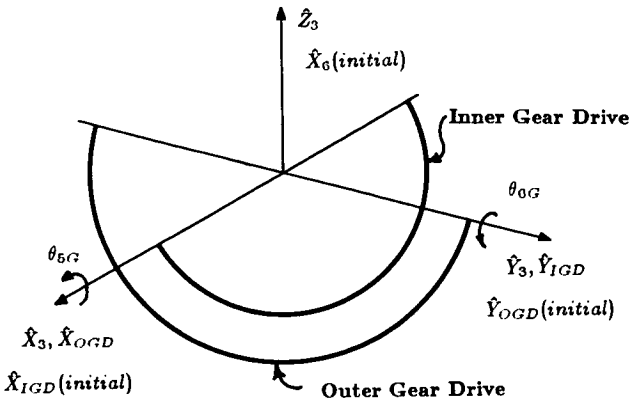

Figure 4
Definition of $\{IGD\}$ and $\{OGD\}$

From Fig. 1, the offset vector from the first to the second universal joint is a length L along $\hat{X}_6$ (denoted $\{^3P_8\}$). The moving axes $\hat{X}_{IGD}$ and $\hat{Y}_{OGD}$ are perpendicular to $\{^3P_8\}$ for any wrist motion.

$$\hat{X}_6 = \frac{\hat{X}_{IGD} \times \hat{Y}_{OGD}}{\left|\hat{X}_{IGD} \times \hat{Y}_{OGD}\right|} \tag{27}$$

The terms for Eq. 27 follow, expressed in $\{3\}$.

$$^3\hat{X}_{IGD} = [^3_{IGD}R]\ ^{IGD}\hat{X}_{IGD} = \begin{Bmatrix} c_{6G} \\ 0 \\ -s_{6G} \end{Bmatrix} \tag{27a}$$

$$^3\hat{Y}_{OGD} = [^3_{OGD}R]\ ^{OGD}\hat{Y}_{OGD} = \begin{Bmatrix} 0 \\ c_{5G} \\ s_{5G} \end{Bmatrix} \tag{27b}$$

$$^3\hat{X}_6 = [^3_6R]\ ^6\hat{X}_6 = \begin{Bmatrix} K1 \\ K2 \\ c_5c_6 \end{Bmatrix} \tag{27c}$$

Substituting these terms yields three scalar equations relating the gear bails and universal joint angles.

$$\frac{c_{5G}s_{6G}}{M} = c_4s_6 + s_4s_5c_6 = K1 \tag{28a}$$

$$\frac{-s_{5G}c_{6G}}{M} = s_4s_6 - c_4s_5c_6 = K2 \tag{28b}$$

$$\frac{c_{5G}c_{6G}}{M} = c_5c_6 \tag{28c}$$

$$M = \sqrt{cos^2\theta_{5G} + sin^2\theta_{5G}cos^2\theta_{6G}} \tag{28d}$$

Equations 28a - 28c are used to find the mappings $F2$ and $I2$.

The angle θ_4 does not have a gear bail; the $F2$ mapping is identity.

$$\theta_4 = \theta_{4G} \tag{29}$$

Using Eq. 29 in Eqs. 28a, b, and c, the following equations result.

$$A = \frac{c_{5G}s_{6G}}{Mc_{4G}} = s_6 + t_{4G}s_5c_6 \tag{30a}$$

$$B = \frac{-s_{5G}c_{6G}}{Mc_{4G}} = t_{4G}s_6 - s_5c_6 \tag{30b}$$

$$C = \frac{c_{5G}c_{6G}}{M} = c_5c_6 \tag{30c}$$

The $sin\theta_5$ term is eliminated from Eqs. 30a and b to solve for θ_6.

$$\theta_6 = sin^{-1}(u) \qquad u = \left[\frac{A + Bt_{4G}}{1 + t_{4G}^2}\right] \tag{31}$$

The inverse sine function yields θ_6 and $\pi - \theta_6$; the latter is out of the motion range of the Omni-Wrist. With θ_6 known, the solution for θ_5 comes from Eq. 30c.

$$\theta_5 = cos^{-1}(v) \qquad v = \left[\frac{C}{c_6}\right] \tag{32}$$

The inverse cosine function solution is $\pm\theta_5$. Since both results are potentially in the motion range of the Omni-Wrist, this ambiguity must be resolved by choosing the θ_5 sign which satisfies Eq. 30b. Map $F2$ is unique.

The mapping $I2$ solves for the gear bail angles given the universal joint angles. The θ_{4G} mapping is Eq. 29. The remaining gear bail angles are found by dividing Eqs. 28b and 28a by Eq. 28c.

$$\theta_{5G} = tan^{-1}(w) \qquad w = \left[\frac{-s_4s_6 + c_4s_5c_6}{c_5c_6}\right] \tag{33a}$$

$$\theta_{6G} = tan^{-1}(q) \qquad q = \left[\frac{c_4s_6 + s_4s_5c_6}{c_5c_6}\right] \tag{33b}$$

Both results from the inverse tangent function are mathematically correct, due to symmetry. However, considering angular limits of the Omni-Wrist, only quadrant I or IV results are admissible. Therefore, the inverse map $I2$ is unique.

Omni-Wrist Velocity Kinematics

Figure 5 shows the three forward and inverse maps relating the four levels of Omni-Wrist velocity parameters. The forward velocity problem finds the cartesian rates given the actuator joint rates, using maps $FV1, FV2$, and $FV3$. The inverse velocity problem accepts $\{^8\omega_8\}$ and calculates the actuator joint rates via maps $IV1, IV2$, and $IV3$.

The velocity maps $FV3$ and $IV1$ are Eqs. 21 and 22, and Eq. 24, respectively. The remaining Omni-Wrist velocity solutions are presented below.

Velocity Maps $FV1$ and $IV3$

The map $FV1$ is a time derivative of Eqs. 26; $IV3$ is the inverse of Eqs. 34.

$$\dot{\theta}_{4G} = N_1\dot{\theta}_{4A} \tag{34a}$$

$$\dot{\theta}_{5G} = N_2\dot{\theta}_{5A} \tag{34b}$$

$$\dot{\theta}_{6G} = N_3\dot{\theta}_{6A} \tag{34c}$$

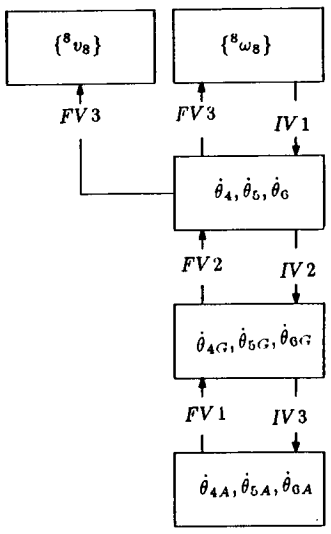

Figure 5
Velocity Mappings

Velocity Maps $FV2$ and $IV2$

The map $FV2$ is a time derivative of $F2$, Eqs. 29, 31, and 32. The angular rate $\dot\theta_6$ is required for the $\dot\theta_5$ calculation.

$$\dot\theta_4 = \dot\theta_{4G} \tag{35}$$

$$\begin{aligned}
\dot\theta_6 &= \frac{1}{\sqrt{1-u^2}}\frac{du}{dt} \\
\frac{du}{dt} &= (Bc2\theta_{4G} - As2\theta_{4G})\dot\theta_{4G} + c_{4G}^2\dot A + c_{4G}s_{4G}\dot B \\
\dot A &= Q\left[t_{4G}c_{5G}s_{6G}\dot\theta_{4G} - s_{5G}s_{6G}\dot\theta_{5G} + c_{5G}c_{6G}\dot\theta_{6G} - \frac{c_{5G}s_{6G}}{M}\dot M\right] \\
\dot B &= Q\left[-t_{4G}s_{5G}c_{6G}\dot\theta_{4G} - c_{5G}c_{6G}\dot\theta_{5G} + s_{5G}s_{6G}\dot\theta_{6G} + \frac{s_{5G}c_{6G}}{M}\dot M\right] \\
Q &= \frac{1}{Mc_{4G}} \\
\dot M &= \frac{-s_{5G}s_{6G}}{\sqrt{1-s_{5G}^2s_{6G}^2}}\left[c_{5G}s_{6G}\dot\theta_{5G} + s_{5G}c_{6G}\dot\theta_{6G}\right]
\end{aligned} \tag{36}$$

$$\begin{aligned}
\dot\theta_5 &= \frac{-1}{\sqrt{1-v^2}}\frac{dv}{dt} \\
\frac{dv}{dt} &= \frac{1}{c_6}\left[Ct_6\dot\theta_6 + \dot C\right] \\
\dot C &= \frac{-1}{M}\left[s_{5G}c_{6G}\dot\theta_{5G} + c_{5G}s_{6G}\dot\theta_{6G} + \frac{c_{5G}c_{6G}}{M}\dot M\right]
\end{aligned} \tag{37}$$

The inverse map $IV2$ is a time derivative of $I2$, Eqs. 33a and 33b. The mapping for $\dot\theta_{4G}$ is Eq. 35.

$$\begin{aligned}
\dot\theta_{5G} &= \frac{1}{1+w^2}\frac{dw}{dt} \\
\frac{dw}{dt} &= \frac{-1}{c_5}(c_4t_6 + s_4s_5)\dot\theta_4 + \frac{1}{c_5^2}(c_4 + s_4s_5t_6)\dot\theta_5 - \frac{1}{c_5c_6^2}(s_4)\dot\theta_6
\end{aligned} \tag{38}$$

$$\begin{aligned}
\dot\theta_{6G} &= \frac{1}{1+q^2}\frac{dq}{dt} \\
\frac{dq}{dt} &= \frac{1}{c_5}(c_4s_5 - s_4t_6)\dot\theta_4 + \frac{1}{c_5^2}(s_4 + c_4s_5t_6)\dot\theta_5 + \frac{1}{c_5c_6^2}(c_4)\dot\theta_6
\end{aligned} \tag{39}$$

The derivatives Eqs. 36, 38, and 39 hold for the angle range $\frac{-\pi}{2}$ to $\frac{\pi}{2}$. The sign of $\dot\theta_5$ in Eq. 37 is positive when $-\pi < \theta_5 < 0$.

EXAMPLES

This section presents two examples to demonstrate the equations derived in this paper. The first example deals with the forward and inverse position and velocity problems for the general double universal joint robot wrist mechanism. The second presents forward and inverse position and velocity results for the Omni-Wrist. The dimensions used in this section are $mm, degrees, \frac{mm}{s}$, and $\frac{rad}{s}$.

Example 1
Forward Position

Given $\theta_4 = 120.0°, \theta_5 = -25.0°, \theta_6 = 10.0°$, and $L = 41$, $[{}^3_8T]$ is calculated using Eq. 3.

$$[{}^3_8T] = \begin{bmatrix} -0.494 & -0.798 & -0.345 & -18.3 \\ -0.452 & -0.103 & 0.886 & -2.4 \\ -0.743 & 0.593 & -0.310 & 36.6 \\ 0 & 0 & 0 & 1 \end{bmatrix} \tag{40}$$

Inverse Position

Given $[{}^3_8R]$ from Eq. 40 three universal joint angles are calculated with Eqs. 14, 16, and 17; the four solutions are formed from Table II.

Table III Inverse Position Solutions

Solution	θ_4	θ_5	θ_6
1	120.0	-25.0	10.0
2	120.0	-25.0	190.0
3	120.0	155.0	-10.0
4	120.0	155.0	170.0

Forward Velocity

Given $\dot\theta_4 = 1.0, \dot\theta_5 = 2.0, \dot\theta_6 = 3.0$, and $L = 41$, $\{^8\omega_8\}$ and $\{^8v_8\}$ are calculated using Eqs. 21 and 22.

$$\{^8\omega_8\} = \begin{Bmatrix} 4.4 \\ 3.7 \\ 3.6 \end{Bmatrix} \qquad \{^8v_8\} = \begin{Bmatrix} -80.0 \\ -10.0 \\ 100.0 \end{Bmatrix} \tag{41}$$

Inverse Velocity (Resolved Rate)

Given $\{^8\omega_8\}$ from Eq. 41, $\dot\theta_4 = 1.0, \dot\theta_5 = 2.0, \dot\theta_6 = 3.0$, are calculated using Eq. 24.

Example 2
Forward Position

Given the actuator angles, the gear bail angles, universal joint angles, and $[{}^3_8T]$ are calculated successively, using maps $F1, F2$, and $F3$. Example 1 presents the $F3$ result.

$$\{\theta_A\} \overset{F1}{\Longrightarrow} \{\theta_G\} \overset{F2}{\Longrightarrow} \{\theta\}$$

$$\begin{Bmatrix} -21060.0 \\ 959.0 \\ 5852.0 \end{Bmatrix} \quad \begin{Bmatrix} 120.0 \\ 3.7 \\ -26.6 \end{Bmatrix} \quad \begin{Bmatrix} 120.0 \\ -25.0 \\ 10.0 \end{Bmatrix} \tag{42}$$

Inverse Position

Given $[{}^3_8R]$ from Eq. 40, the universal joint, gear bail, and actuator angles are calculated using $I1, I2$, and $I3$. Example 1 presents $I1$. Considering angular limits, only the first solution in Table III is reachable. The inverse maps $I2$ and $I3$ are the reverse of maps $F2$ and $F1$ in Eq. 42, respectively.

Forward Velocity

Given the actuator rates, the gear bail, universal joint, and cartesian rates are calculated with the mappings $FV1, FV2$, and $FV3$. Example 1 gives $FV3$.

$$\{\dot{\theta}_A\} \overset{FV1}{\Longrightarrow} \{\dot{\theta}_G\} \overset{FV2}{\Longrightarrow} \{\dot{\theta}\}$$

$$\begin{Bmatrix} -175.5 \\ -907.2 \\ -88.0 \end{Bmatrix} \quad \begin{Bmatrix} 1.0 \\ -3.5 \\ 0.4 \end{Bmatrix} \quad \begin{Bmatrix} 1.0 \\ 2.0 \\ 3.0 \end{Bmatrix} \tag{43}$$

Inverse Velocity (Resolved Rate)

Given $\{{}^8\omega_8\}$ from Eq. 41, the universal joint, gear bail, and actuator rates are found, using $IV1, IV2$, and $IV3$. Example 1 presents $IV1$. The mappings $IV2$ and $IV3$ are the reverse of $FV2$ and $FV1$ in Eq. 43, respectively.

CONCLUSION

This paper presents kinematic equations for control of a double universal joint robot wrist. The forward and inverse position and velocity problems were solved. The Omni-Wrist equations were developed in detail. This wrist has four levels of kinematic parameters. Three forward and inverse position and velocity maps relating these parameters were presented. These equations relate the hand coordinate frame to the wrist base coordinate frame, and are sufficient for controlling the wrist standing alone. All pertinent kinematic equations were derived; any specific control algorithm will not require all of the equations. All Omni-Wrist solutions are unique. The Omni-Wrist is completely singularity-free throughout its range of motion.

The equations of this paper have been verified by computer simulation. As demonstrated by the examples, the inverse solutions validate the forward solutions. Experimental work using the Omni-Wrist is planned to further validate the equations.

The offset, L, between the two universal joints complicates the inverse kinematics problems when the double universal joint robot wrist is attached to a manipulator arm. The wrist coordinate frames are not all colocated, which prevents decoupling of the hand coordinate frame position and orientation. For a three degree of freedom manipulator arm carrying the double universal robot wrist, the inverse position problem involves six transcendental equations, coupled in the six unknowns. The associated Jacobian matrix is fully populated, which means the hand linear velocity depends on the wrist rates in addition to the first three joint rates. The kinematics of a manipulator using the double universal joint robot wrist is a subject for future research.

REFERENCES

Barker, L.K., "Theoretical Three- and Four-Axis Gimbal Robot Wrists", NASA Technical Paper 2564, May 1986.

Craig, J.J., *Introduction to Robotics: Mechanics and Control*, Addison Wesley Publishing Co., Reading, MA, 1988.

Mabie, H.H., and Reinholtz, C.F., *Mechanisms and Dynamics of Machinery*, John Wiley & Sons, New York, 1987.

McKinney, W.S.,"Kinematics of Hooke Universal Joint Robot Wrists", NASA Technical Memorandum 100567, June 1988.

Milenkovic, Veljko, "New Nonsingular Robot Wrist Design", *Robots 11 Conference Proceedings RI/SME*, Chicago, IL, April 1987, pp. 13.29-13.42.

Rosheim, M.E., *Robot Wrist Actuators*, John Wiley & Sons, New York, 1989.

Rosheim, M.E., "Singularity-Free Hollow Spray Painting Wrists", *Robots 11 Conference Proceedings RI/SME*, Chicago, IL, April 1987, pp. 13.7-13.28.

Rosheim, M.E., "Four New Robot Wrist Actuators", *Robots 10 Conference Proceedings RI/SME*, Chicago, IL, April 1986, pp. 8.1-8.45.

Trevelyan, J.P., et. al., "ET: A Wrist Mechanism Without Singular Positions", *The International Journal of Robotics Research*, Winter, 1986, pp. 71-85.